ISSN 1054-660X, Laser Physics, 2011, Vol. 21, No. 11, pp. 1–6.

Polarization Manipulated Solid-State Lasers with Crystalline-Orientations[1]

J. Dong*, J. Ma, and Y. Y. Ren

Department of Electronics Engineering, School of Information Science and Technology, Xiamen University, Xiamen 361005, China

*e-mail: jdong@xmu.edu.cn

Received June 7, 2011; in final form, June 9, 2011

Abstract—The polarization states of ⟨111⟩-cut Yb:YAG crystal microchip lasers were investigated by pumped with the elliptically polarized pump beam from fiber-coupled laser-diode. The manipulated polarized lasers were achieved in laser-diode pumped Yb:YAG microchip laser by controlling the crystalline-orientations in ⟨111⟩-growth Yb:YAG crystal. Generally elliptically polarized lasers were obtained in laser-diode pumped Yb:YAG microchip lasers. However, crystalline-orientation manipulated linearly polarized laser was obtained when six different sites with different crystalline orientations were set to parallel to the major axis direction of the elliptically polarized pump beam. Six different sites in Yb:YAG crystal were separated with 30° and 90°, which were responsible for the linearly polarized laser oscillations. Circularly polarized lasers were observed when a Yb:YAG crystal was aligned to a special position between two sites responsible for linearly polarized laser oscillation. Effects of the polarization states of pump source on the laser polarization states of Yb:YAG microchip lasers and polarization direction of different polarized lasers with respect to Yb:YAG crystal rotation was addressed.

DOI: 10.1134/S1054660X11210043

1. INTRODUCTION

Laser sources with desirable polarization states are of great interest for many applications. For example, linear polarized laser sources are of great important in nonlinear frequency conversion [1], materials microstructure analysis [2], laser beam combining, and so on, circular polarized laser sources are of high interest in chemistry and biology for detecting molecules exhibiting circular dichroism [3, 4]. However, lasers are mostly linearly polarized, which is determined by the optical selection rules of the gain media which usually exhibit anisotropic properties [5, 6]. Other states of polarizations proved difficult to achieve.

Conventionally, manipulation of the polarization states of a laser output is conducted externally using bulky and expensive optical components such as beam-splitting polarizer and wave plates. These optical components make the laser system more complex and difficult to maintain. Some special design of coatings and apertures were used to obtain different polarization states of laser output [7, 8], especially recently reported polarization manipulated laser output from a semiconductor laser with integrated plasmonic polarizers on the laser emission facet [9]. It is well-known that the beam quality is not good in semiconductor lasers and pulsed lasers are difficult to achieve. Microchip lasers offer another effective way to achieve good beam quality and combine with other optical components to achieve pulsed lasers and efficient nonlinear frequency conversion. However, polarizations manipulation of microchip lasers has to be made using laser crystals with anisotropic optical properties and using external force such as special coatings, changing temperature and pressure of crystals with isotropic optical properties. Although different polarization states can be achieved with special coating designs in microchip lasers, the multi-layer coating design is weak under the high laser intensity and is difficult to maintain high power operation.

Yttrium aluminum garnet (YAG) is an attractive laser host material because of its excellent thermal, chemical and mechanical properties [10]. Yb:YAG has been a promising candidate for high-power laser-diode pumped solid-state lasers [11] owing to its unique properties of easy growth of high doped concentration crystal. Temperature dependent emission cross section of Yb:YAG materials [12] provides another flexible design for efficient operation of cryogenically-cooled Yb:YAG lasers [13]. Highly efficient intracavity frequency-doubled Yb:YAG lasers have been demonstrated recently [14–17]. Frequency doubling of Yb:YAG lasers at 515 nm matches the highest power line of Ar-ion lasers, thereby leading to the possibility of an all solid-state replacement [18, 19]. Efficient Cr,Yb:YAG self-Q-switched laser performance have been achieved by bonding Yb:YAG crystal [20]. In the past decade, high quality transparent Yb:YAG ceramics have been fabricated and efficient laser operation has been demonstrated [21]. Comparative investigation of laser performance of Yb:YAG ceramics and crystals has been done and results show that Yb:YAG ceramics provide comparable or better laser perfor-

[1] The article is published in the original.

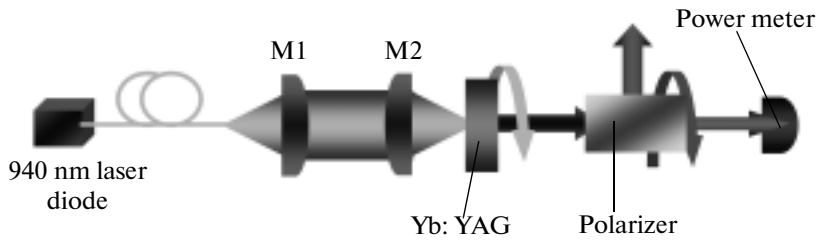

Fig. 1. Schematic diagram of experimental setup for measuring crystalline-orientation dependent polarization of continuous-wave Yb:YAG microchip laser. M1 and M2 are the focus lens used in collimating pump beam.

mance comparing to their counterpart Yb:YAG crystals doped with different Yb concentrations[22]. Efficient laser performance of heavy doped Yb:YAG ceramics has been demonstrated recently [23, 24]. High power laser-diode pumped Yb:YAG lasers based on Yb:YAG ceramics and crystals have been demonstrated with different laser resonator configuration [25–28]. Yb:YAG ceramics have been successfully used to generate very-high order Laguerre–Gaussian modes by using a simple short-focus plano-convex glass lens [29] and circular modes by using a spherical intracavity lens [30]. Efficient laser performance of Yb:YAG crystals at room temperature without active cooling of Yb:YAG gain medium has been obtained with high pump power intensity at room temperature [31, 32]. Efficient CW and Q-switched laser performance of other ytterbium doped garnets such as Yb:LuAG and Yb:$Y_3Sc_2Al_5O_{12}$ has also been demonstrated [33–35]. Therefore, it is very important to find an easy way to manipulate polarization states in rare-earth doped YAG microchip lasers. Recently crystalline-orientation self-selected linearly polarization has been observed in Yb:YAG microchip lasers [36]. However, the relationship between linearly polarized lasers and crystal orientation of Yb:YAG crystal have not known well, and at the same time the effect of polarization states of commercial available laser diode on the polarization state has not been investigated. Actually, the polarization state of pump beam is a very important factor in polarization manipulated microchip laser.

In this paper, manipulation of polarization states by aligning crystal orientations of Yb:YAG crystal with the major axis direction of elliptically polarized fiber-coupled laser-diode was achieved in laser-diode pumped Yb:YAG microchip lasers. Linear, elliptical and circular polarization states of continuous-wave laser output was observed by aligning the different orientation crystal sites within the major axis direction of elliptically polarized pumped beam from fiber-coupled laser-diode. The effect of the polarization state of pump source on the laser performance was investigated and found the laser polarization state has certain relationship with the polarization state of pump source. However, the major factor for polarization manipulated lasers is the crystalline-orientations of three-fold symmetry of Yb:YAG crystal. The polarization direction of Yb:YAG microchip laser under different crystalline orientations was discussed with respect to the rotation angles of Yb:YAG crystal along laser propagation direction.

2. EXPERIMENTAL SETUP

A schematic diagram of experimental setup for crystalline-orientations manipulated polarization states of laser-diode pumped microchip Yb:YAG lasers is shown in Fig. 1. An 1-mm-thick, plane-parallel Yb:YAG single crystal plate doped with 10 at % Yb ions was used as gain media. Yb:YAG crystals were grown by Czochralski (CZ) method along the [111] direction. One surface of the Yb:YAG plate perpendicular to the [111] crystalline axis is anti-reflection-coated at 940 nm and high reflection coated at 1030 nm to act as a cavity mirror of the laser. The other surface of the Yb:YAG is coated with total reflection at 940 nm to increase the absorption of pump power and partially coated with reflection of 90% at 1030 nm to act as the other cavity mirror of the laser. The Yb:YAG crystal was held together with a copper holder which can be rotated around the axis of laser propagation direction. The Yb:YAG sample is rotated counter-clockwise in the step of 5°. A fiber-coupled 940 nm laser-diode (LIMO35-F200-DL940) with a core diameter of 200 μm and numerical aperture of 0.22 was used as the pump source. Two lenses with 8-mm focal length were used to collimate and focus the pump beam on the crystal rear surface and to produce a pump light footprint in the crystal of about 160 μm in diameter. The Yb:YAG microchip laser was operated at room temperature without active cooling of the active element. The polarization states of Yb:YAG microchip lasers and laser-diode were measured by using a Glan–Thomson prism and a power meter.

3. RESULTS AND DISCUSSION

The polarization states of laser-diode pump beam used in the experiments were determined before the polarization states of Yb:YAG microchip lasers were measured. The polarization state of pump beam from fiber-coupled laser-diode was measured and found

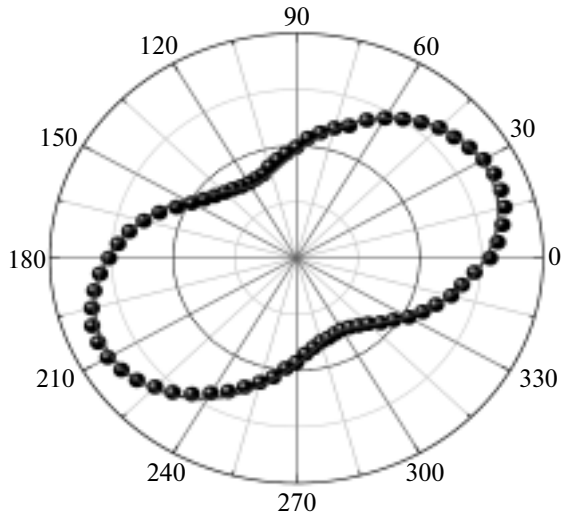

Fig. 2. Measured polarization state of fiber-coupled laser-diode used in the experiment, solid symbols are the experimental data, solid-line is the fitting with elliptical function.

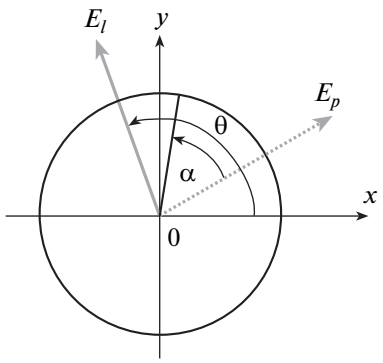

Fig. 3. Schematic diagram of crystal rotation and polarization of Yb:YAG microchip laser. E_p and E_l are the polarization direction of pump and laser beam; α is the rotation angle of Yb:YAG crystal with respect to the polarization direction of pump beam, θ is the polarization direction with respect to the *x*-axis.

that the pump beam exhibits elliptical polarization. The major axis direction of the elliptically polarized pumped beam is 28° with respect to the *x*-axis of polarizer, as shown in Fig. 2. And the ratio of major axis to the minor axis of the elliptically polarized pump beam was determined to be 1.5.

First, the relationship between linearly polarization states of Yb:YAG microchip lasers and crystalline-orientations in Yb:YAG crystal was determined by measuring the polarization states under different crystal orientations through rotating Yb:YAG crystal counterclockwise. Under longitudinal pumping along [111] direction of Yb:YAG crystal, the laser propagates along the same direction, the electronic field victor is perpendicular to [111] direction and is in (111) plane. The relationship between crystalline orientations in Yb:YAG crystal and the polarization states of ⟨111⟩-cut Yb:YAG crystal microchip lasers was investigated by rotating Yb:YAG crystal along [111] direction. Figure 3 shows the schematic rotation of Yb:YAG crystal and the possible polarization direction of Yb:YAG lasers in (111) plane of Yb:YAG crystal. *x* and *y* are the axes of Glan–Thomson polarizer. α is the rotation angle of Yb:YAG crystal with respect to the polarization direction of pump beam and the start rotation angle of Yb:YAG crystal is set to be parallel to the major axis direction of the elliptically polarized pump beam, E_p. θ is the possible polarization direction of Yb:YAG lasers, E_l.

The $Y_3Al_5O_{12}$ (YAG) crystal has cubic symmetry with space-group O_h^{10} (*Ia*3*d*) and eight formula units per unit cell. The Y^{3+} ions occupy six crystallographically equivalent but orientationally inequivalent sites with dodecahedral point symmetry (D_2 point group). For Yb:YAG crystal, Yb^{3+} ions normally substitute for the Y^{3+} ions and experience the same D_2 symmetry. Owing to the radius of Yb^{3+} ions is close to that of Y^{3+} ions, the doping concentration of Yb^{3+} ions can reach up to 100 at % to form YbAG crystal. Figure 4 schematically shows the three-fold symmetry of Yb:YAG crystal, six sites with different orientations in cubic YAG doped with Yb^{3+} lasants and their relationship to the axes *XYZ* of the unit cell, where *x*, *y*, and *z* are labels for the local axes for the D_2 symmetry of site 1. The local axes *x* are parallel to the cubic axes of the unit cell, while the axis *y* and *z* are parallel to the face diagonals. There are six local sites in Yb:YAG crystal. The transition dipoles necessarily lie along either *x*, *y*, or *z*, depending on the electronic states, according to the selection rules for electric and magnetic dipole transitions in D_2 symmetry. Since the local *x*, *y*, *z* axes of the six sites are oriented differently from each other, the six sets of dipoles (arising from the six sets of Yb^{3+} sites) will also be oriented differently, even though the sites are crystallographically equivalent. The pump and laser beam is along ⟨111⟩ direction of Yb:YAG crystal, electric states of laser beam have to be within (111) plane.

The polarization states manipulation of Yb:YAG microchip continuous-wave laser was done by choosing the different crystalline-orientations in Yb:YAG crystal. In sites with D_2 symmetry, the intensities of transition dipole moment along the three inequivalent Cartesian axes are different; consequently, polarized pump light will drive various sites differently. Similarly, the laser fields with a specific polarization will "burn down" the population inversion differently, therefore, different polarization states will be observed.

For convenience, site 1 of Yb:YAG crystal (as shown in Fig. 4) was aligned to within the major axis direction of elliptically polarized pump beam and was

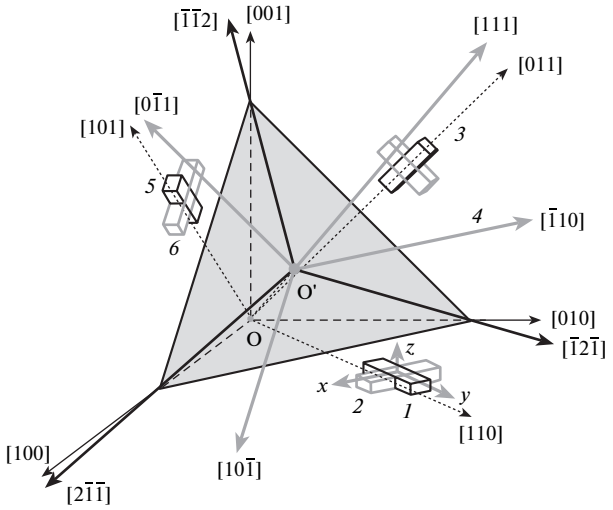

Fig. 4. Orientation of the six orientationally inequivalent sites of the Yb^{3+} ions in YAG crystal lattice. Each lozenge-shape parallelepiped represents the local D_2 symmetry for a subset of sites. The x, y, and z axes are the local axes of site 1. Experiments were carried out with light propagating along the [111] axis.

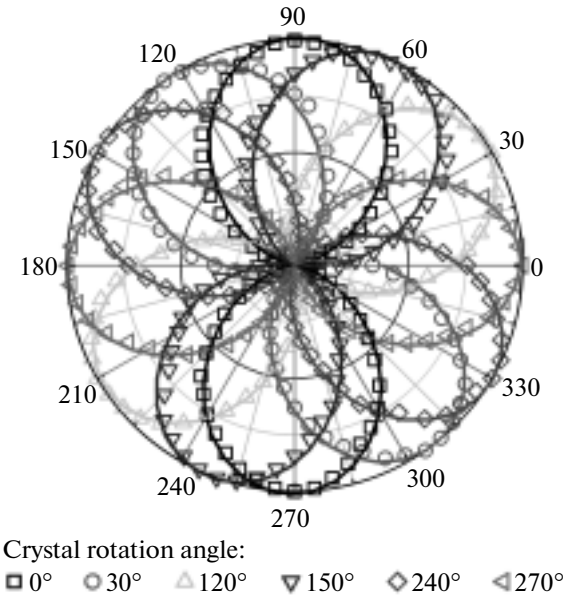

Fig. 5. Linear polarization of continuous-wave Yb:YAG microchip laser as a function of polarizer rotation angle for six different crystal rotation angles along [111] direction of Yb:YAG crystal. The symbols show the measured data and solid lines show the cosine square function fitting.

denoted as the start point of Yb:YAG crystal rotation angle (as shown in Fig. 3). In this case, the crystalline-orientation of [$\bar{1}\bar{1}$2] in (111) plane or the project of [110] on (111) plane of Yb:YAG crystal was set to be parallel to the major axis direction of the elliptically polarized pump beam. When Yb:YAG laser oscillates, the polarization state of the Yb:YAG microchip laser was measured and found that polarization state is linearly polarized and the polarization direction was measured to be 90° with respect to the x-axis of Glan–Thomson polarizer, as shown in Fig. 5. Further rotating of Yb:YAG crystal counterclockwise, linearly polarized laser output was obtained when site 6 of Yb:YAG crystal (as shown in Fig. 4) was aligned to within the major axis direction of the elliptically polarized pump beam. At this case, Yb:YAG crystal was rotated 30° counterclockwise and [10$\bar{1}$] in (111) plane was parallel to the major axis direction of the elliptically polarized pump beam. The direction of linearly polarized laser was measured to be 120° with respect to x-axis as shown in Fig. 5. Linearly polarized laser output was observed when the Yb:YAG crystal was further rotated 90° to 120° with respect to the major axis direction of the elliptically polarized pump beam, the direction of linearly polarized laser was measured to be 35° (or 215 degrees). At this crystal orientation, the site 5 of Yb:YAG crystal was aligned to be parallel to the major axis direction of the elliptically polarized pump beam, as shown in Fig. 4. The linearly polarized laser output was observed in laser-diode pumped Yb:YAG microchip lasers when the Yb:YAG crystal was rotated to 150°, 240°, and 270° with respect to the major axis direction of the elliptically polarized pump beam. At these crystal orientations, the sites 4, 3, and 2 of Yb:YAG crystal was aligned to be within the major axis direction of the elliptically polarized pump beam, respectively. The direction of linearly polarized lasers were measured to be 250° (or 70°), 330 degrees (150°), and 360° (or 0°), respectively. The observed linearly polarized lasers under different sites of Yb:YAG crystal pumped with elliptically polarized pump beam are separating 30 and 90°, exhibiting three-fold symmetry, which is in good agreement with our previous results of crystalline-orientation self-selected linearly polarization Yb:YAG microchip laser [36] and the three-fold symmetry of rare-earth doped YAG crystals [37, 38]. From Figs. 4 and 5, we can see that six orientationally different crystal sites are responsible for the linearly polarization oscillation in Yb:YAG microchip lasers under elliptically polarized pump beam when these sites of Yb:YAG are aligned to be within the major axis direction of the elliptically polarized pump beam. From the crystal field of three-fold symmetry of Yb:YAG crystal (as shown in Fig. 4) and the linearly polarized laser output under different crystal orientations (as shown in Fig. 5), the linearly polarized laser output from laser-diode pumped Yb:YAG microchip lasers was attributed to the dipole moment from these different sites when these six different crystal orientation sites was aligned to be parallel to the major axis direction of the elliptically polarized pump beam.

Except for six sites of Yb:YAG crystal responsible for linearly polarized laser output, generally, the laser output of Yb:YAG microchip lasers was measured to

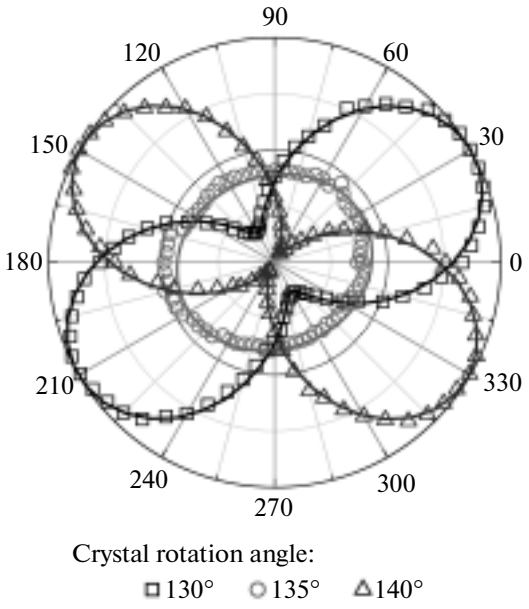

Fig. 6. Observed elliptical and circular polarization laser output. The symbols show the measured data and solid lines show the cosine square function fitting.

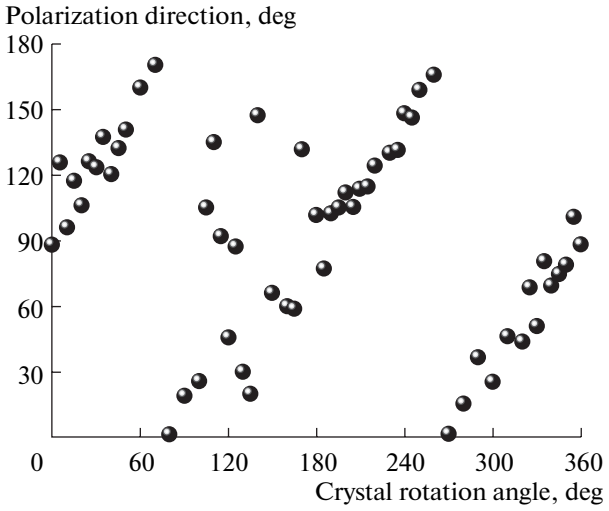

Fig. 7. Measured polarization direction of Yb:YAG microchip laser at different crystal rotation angles. The polarization direction of pump source is along 28° with respect to the *x*-axis.

be elliptically polarized. Most interesting phenomena in present laser-diode pumped Yb:YAG microchip laser experiment is that circular polarization was also observed when the Yb:YAG crystal was rotated 135°, at this position, the major axis direction of the elliptical polarized pump laser was aligned between two crystal sites (site 5 and site 4), which are responsible for linearly polarized laser output. Figure 6 shows some typical elliptical polarized states and one circular polarized state obtained in Yb:YAG microchip lasers when the Yb:YAG crystal was rotated to 130°, 135°, and 140°, which is between two linearly polarization states at 120° and 150°. The elliptical polarization state is the general polarization in laser-diode pumped Yb:YAG microchip lasers, linearly polarization and circular polarization state are two special cases requiring the transition dipole moment of Yb:YAG crystal in (111) plane satisfying the three-fold symmetry of D_2 in YAG crystal. Therefore, the manipulation of polarization states in laser-diode pumped Yb:YAG microchip lasers is achieved by adjusting the crystal orientations in Yb:YAG crystal.

Polarization direction of different polarization states was also measured when Yb:YAG crystal was rotated. The polarization direction of Yb:YAG microchip lasers was plotted as a function of Yb:YAG crystal rotation angle, as shown in Fig. 7. The direction of polarization increases linearly with rotation angle of Yb:YAG crystal. This mean that the direction of different polarization states is kept constant with respect to the sites of Yb:YAG crystal. When the polarization state of elliptically polarized pump beam is kept the same direction, the polarization direction of microchip laser increases linearly with rotation angles of Yb:YAG crystal. The linear relationship between polarization direction of Yb:YAG microchip lasers and the rotation angle of Yb:YAG crystal shows that the polarization states of elliptically polarized pump beam have little effect on the polarization states of ⟨111⟩ Yb:YAG microchip lasers. The polarization states of ⟨111⟩ Yb:YAG microchip laser is govern by the different orientations of three-fold symmetry of Yb:YAG crystal. From 120° to 170° of rotating Yb:YAG crystal, the polarization direction does not increase linearly with rotation angle of Yb:YAG crystal. However, the circularly polarized laser output was observed in this region. At present the mechanism of such variation of polarization direction with rotation angle of Yb:YAG crystal is not clear and it will be clarified later.

4. CONCLUSIONS

In summary, we have achieved crystalline-orientation selected polarization states manipulated laser operation in laser-diode pumped microchip Yb:YAG continuous-wave lasers. Elliptically polarized laser output is the general case in laser-diode pumped ⟨111⟩ Yb:YAG microchip lasers. Six linearly polarized laser output were obtained by setting six different orientation sites to be parallel to the major axis direction of elliptically polarized pump beam. Circularly polarized laser output was observed when the crystalline orientation of Yb:YAG crystal was set between sites 4 and 5. The polarization direction of different polarization states from ⟨111⟩ Yb:YAG microchip lasers increases linearly with the rotation angles of Yb:YAG crystal. The polarization direction is kept unchanged with

respect to the crystalline orientation under elliptically polarized laser pumping.

Our experimental results on manipulated polarization states, by choosing different crystalline orientation sites in Yb:YAG crystal open up a variety of further prospects. Having polarization manipulations available that are sufficient for independent combinations allows the design of new set-ups. For example, isotropic passively Q-switched elements could provide pulse modulations, and a crystalline-orientation selected polarization manipulated laser gain medium could realize polarization states manipulation, allowing high pulse energy, high peak power achievable, at the same time keeping desirable polarization through selecting the suitable orientation in rare-earth doped YAG crystals. Furthermore, it might be advantageous to take advantage of the modern transparent ceramic technology and microchip solid-state lasers for numerous proposed applications. It could avoid limitations where rare-earths doped YAG crystals are suggested as the isotropic cubic structure and extra optical elements are needed for polarization manipulation.

ACKNOWLEDGMENTS

This work was supported by the Fundamental Research Funds for the Central Universities (2010121058), Program for New Century Excellent Talents in University (NCET-09-0669), SRF for ROCS, SEM, and a grant from the Ph.D. Programs Foundation of Ministry of Education of China (20100121120019).

REFERENCES

1. A. V. Kir'yanov, V. Aboites, and I. V. Mel'nikov, J. Opt. Soc. Am. B **17**, 1657 (2000).
2. R. Sigel, G. Fytas, N. Vainos, S. Pispas, and N. Hadjichristidis, Science **297**, 67 (2002).
3. J. Ortigoso and M. Rodriguez, Nature Photon. **3**, 685 (2009).
4. H. Ernst, F. Charra, and L. Douillard, Science **279**, 679 (1998).
5. A. W. Tucker, M. Birnbaum, C. L. Fincher, and J. W. Erler, J. Appl. Phys. **48**, 4907 (1977).
6. T. M. Pollak, W. F. Wing, R. J. Grasso, E. P. Chicklis, and H. P. Jenssen, IEEE J. Quantum Electron. **18**, 159 (1982).
7. J. F. Bisson, O. Parriaux, J. C. Pommier, S. Tonchev, and K. Ueda, Appl. Phys. B **85**, 519 (2006).
8. J. L. Li, K. Ueda, M. Musha, L. X. Zhong, and A. Shirakawa, Opt. Lett. **33**, 2686 (2008).
9. N. Yu, Q. J. Wang, C. Pflugl, L. Diehl, and F. Capasso, Appl. Phys. Lett. **94**, 151101 (2009).
10. A. A. Kaminskii, *Laser Crystals* (Springer, Berlin, Heidelberg, New York, 1981).
11. A. Giesen, H. Hugel, A. Voss, K. Wittig, U. Brauch, and H. Opower, Appl. Phys. B **58**, 365 (1994).
12. J. Dong, M. Bass, Y. Mao, P. Deng, and F. Gan, J. Opt. Soc. Am. B **20**, 1975 (2003).
13. J. Kawanaka, Y. Takeuchi, A. Yoshida, S. J. Pearce, R. Yasuhara, T. Kawashima, and H. Kan, Laser Phys. **20**, 1079 (2010).
14. J. Dong, A. Shirakawa, and K. Ueda, Appl. Phys. B: Laser Opt. **85**, 513 (2006).
15. T. Yubing, T. Huiming, C. Hongzhong, and M. Jieguang, Laser Phys. **18**, 15 (2008).
16. H. Z. Cao, F. J. Liu, H. M. Tan, H. Y. Peng, M. H. Zhang, Y. Q. Chen, B. Zhang, B. L. Chen, and C. J. Wang, Laser Phys. **19**, 919 (2009).
17. Y. B. Tian, Z. H. Tian, H. M. Tan, and X. Y. Liu, Laser Phys. **20**, 793 (2010).
18. T. Y. Fan and J. Ochoa, IEEE Photon. Technol. Lett. **7**, 1137 (1995).
19. G. C. Sun, Y. D. Li, M. Zhao, X. Y. Chen, J. B. Wang, and G. B. Chen, Laser Phys. **21**, 883 (2011).
20. J. Y. Zhou, J. Ma, J. Dong, Y. Cheng, K. Ueda, and A. A. Kaminskii, Laser Phys. Lett. **8**, 591 (2011).
21. J. Dong, A. Shirakawa, K. Ueda, H. Yagi, T. Yanagitani, and A. A. Kaminskii, Appl. Phys. Lett. **89**, 091114 (2006).
22. J. Dong, K. Ueda, H. Yagi, A. A. Kaminskii, and Z. Cai, Laser Phys. Lett. **6**, 282 (2009).
23. J. Dong, A. Shirakawa, K. Ueda, H. Yagi, T. Yanagitani, and A. A. Kaminskii, Opt. Lett. **32**, 1890 (2007).
24. A. Pirri, D. Alderighi, G. Toci, and M. Vannini, Laser Phys. **20**, 931 (2010).
25. A. Giesen and J. Speiser, IEEE J. Sel. Top. Quantum Electron. **13**, 598 (2007).
26. C. Stewen, K. Contag, M. Larionov, A. Giessen, and H. Hugel, IEEE J. Sel. Top. Quantum Electron. **6**, 650 (2000).
27. A. G. Wang, Y. L. Li, and X. H. Fu, Laser Phys. Lett. **8**, 508 (2011).
28. Q. Liu, X. Fu, D. Ma, X. Yan, F. He, L. Huang, M. Gong, and D. Wang, Laser Phys. Lett. **4**, 719 (2007).
29. M. P. Thirugnanasambandam, Y. Senataky, and K. Ueda, Laser Phys. Lett. **7**, 637 (2010).
30. Y. Senatsky, J.-F. Bisson, A. Shelobolin, A. Shirakawa, and K. Ueda, Laser Phys. **19**, 911 (2009).
31. J. Dong, A. Shirakawa, K. Ueda, J. Xu, and P. Z. Deng, Appl. Phys. Lett. **88**, 16 (2006).
32. J. Dong, A. Shirakawa, K. I. Ueda, and A. A. Kaminskii, Appl. Phys. B **89**, 359 (2007).
33. J. Dong, K. Ueda, and A. A. Kaminskii, Opt. Express **16**, 5241 (2008).
34. J. Dong, K. Ueda, and A. A. Kaminskii, Opt. Lett. **32**, 3266 (2007).
35. J. Dong, K. Ueda, and A. A. Kaminskii, Laser Phys. Lett. **7**, 726 (2010).
36. J. Dong, A. Shirakawa, and K. Ueda, Appl. Phys. Lett. **93**, 101105 (2008).
37. R. Bayerer, J. Heber, and D. Mateika, Z. Phys. B: Condens. Matter. **64**, 201 (1986).
38. L. Dobrzycki, E. Bulska, D. A. Pawlak, Z. Frukacz, and K. Wozniak, Inorg. Chem. **43**, 7656 (2004).

SPELL: OK